

Neutron Capture and Scattering Measurements at RPI

Y. Danon, E. Liu, A. Daskalakis, B. McDermott, C. Wendorff, K. Ramic

Rensselaer Polytechnic Institute, Troy, NY, 12180



NCSP Meeting, LLNL, March 19, 2015

RPI Nuclear Data Group

RPI Faculty

Prof. Yaron Danon - LINAC Director

Prof. Li Liu

KAPL

Dr. Greg Leinweber

Prof. (Emeritus) Robert C. Block

Dr. Devin Barry

Dr. Michael Rapp

Dr. Tim Donovan

Mr. Brian Epping

Dr. John Burke

Technical Staff

Dr. Ezekiel Blain

Peter Brand

Matt Gray

Martin Strock

Azeddine Kerdoun

Graduate Students

Adam Daskalakis

Brian McDermott

Adam Weltz

Nicholas Thompson

Kemal Ramic

Carl Wendorff

Amanda Youmans

Jesse Brown

BOLD= researcher or graduate students supported by NCSP



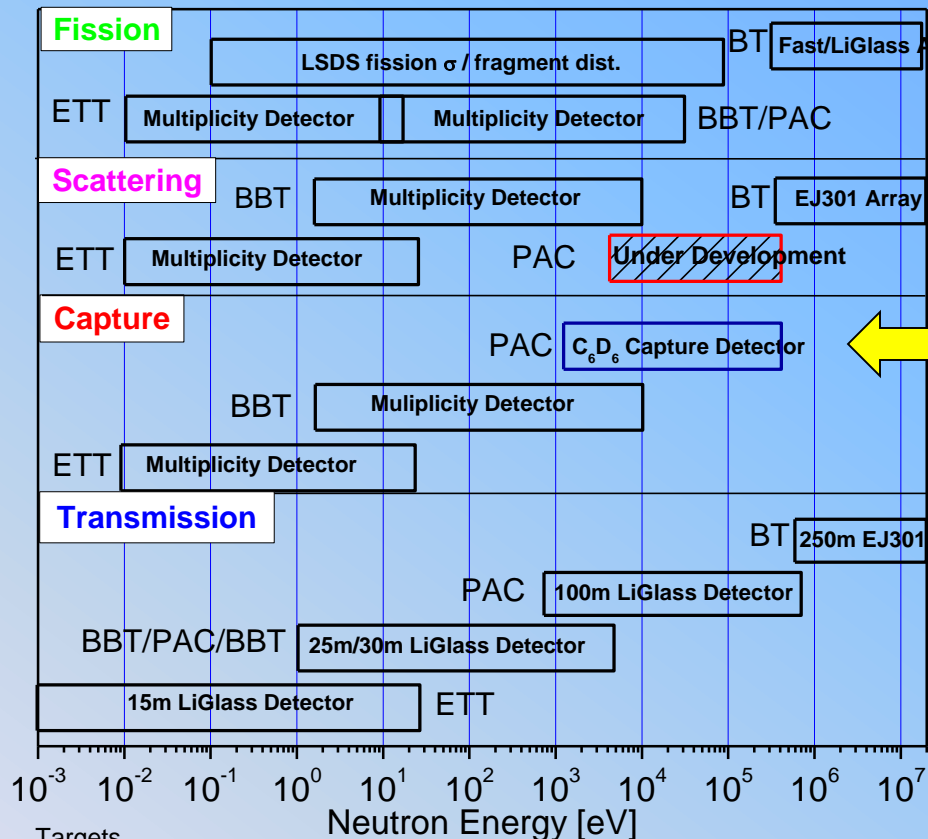
Overview

- **ND-1- Resonance Region Nuclear Data Measurement**
 - Development of a new mid energy capture detector
 - 45m flight path and capture detector are operational, planned energy range from 1 keV to 500 keV
 - Performed measurements of Fe and Ta, demonstrated capture measurements up to 1 MeV.
 - Neutron scattering measurements for Fe
 - 30m flight path, 0.5 MeV to 20 MeV
 - Obtained the ratio of inelastic to 1st state to elastic scattering.
 - Obtained elastic scattering angular data to improve ORNL fit to extend the RRR to 2 MeV
- **ND-2 Thermal Neutron Scattering Measurements**
 - More details in the next talk
- **ND-3 LINAC 2020 Refurbishment and Upgrade Plan**
 - Klystron order was sent to vendor



Capability Development

- Developed Mid energy (1 - 500 keV) capture detector

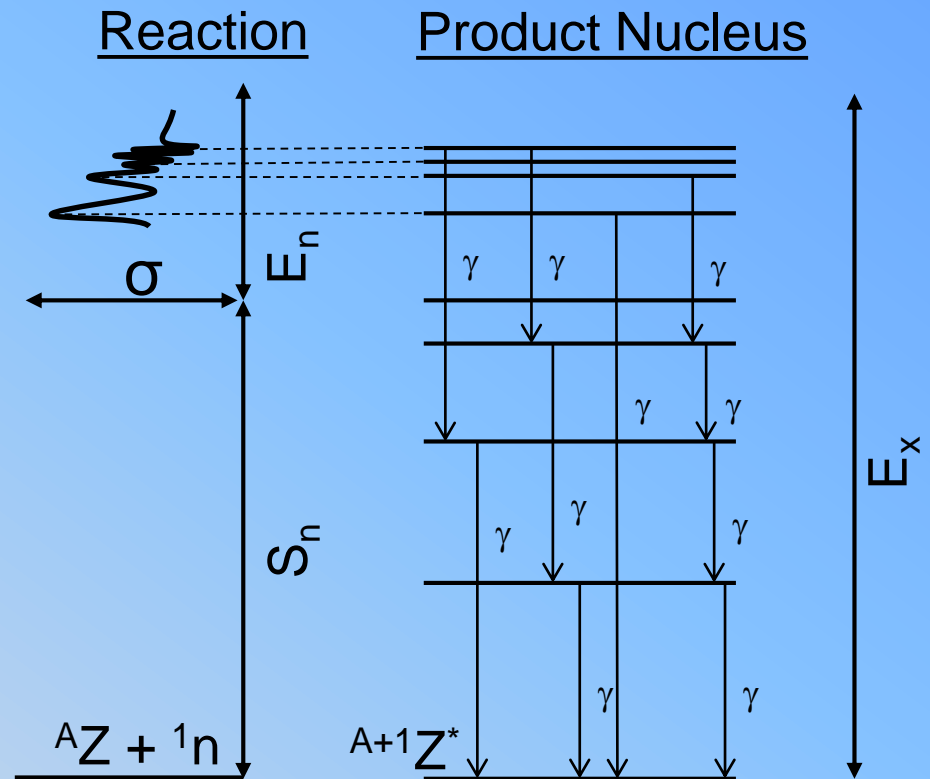


Targets
 ETT- Enhanced Thermal Target
 BBT - Bare Bounce Target
 BT- Bare Target on Axis
 PAC - PacMan Target



Resonance Capture

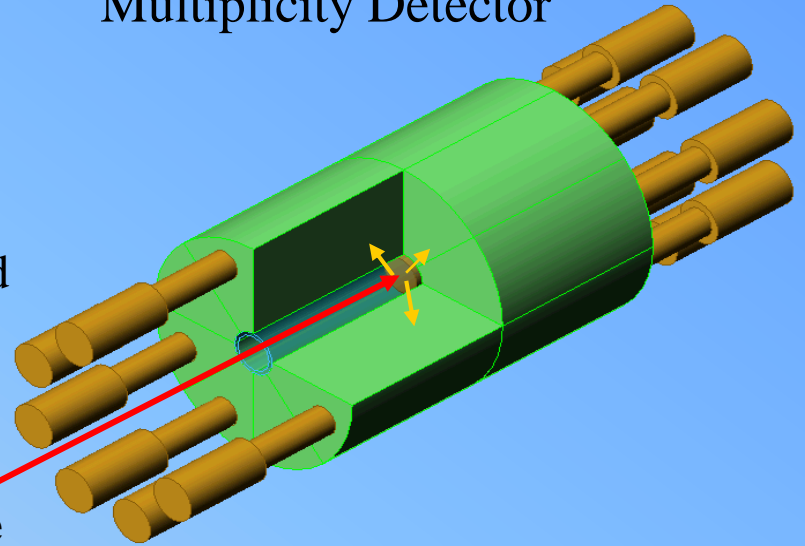
- Resonances represent excited states within the newly formed compound nucleus.
- Following neutron capture the compound nuclide deexcites by emitting a gamma cascade (typically 1-5 gammas).
- The total energy of the gamma is about equals the neutron binding energy (few MeV)
- The multiplicity depends on the nuclide (Z,A) and the resonance spin state (J)



Why New Capture detector

- RPI has a multiplicity Detector
 - $\sim 4\pi$ gamma detector
 - At $E > 2$ keV resonances exhibit much higher scattering than capture cross section
 - Neutron will scatter to the NaI scintillator and produce a capture like gamma cascade
 - Uses a 1 cm thick $^{10}\text{B}_4\text{C}$ liner designed to absorb neutron that scatters from the sample.
 - **Above 2 keV the liner is no longer effective**
 - **This detector is heavily shielded and located on a 25m flight path distance**

Multiplicity Detector

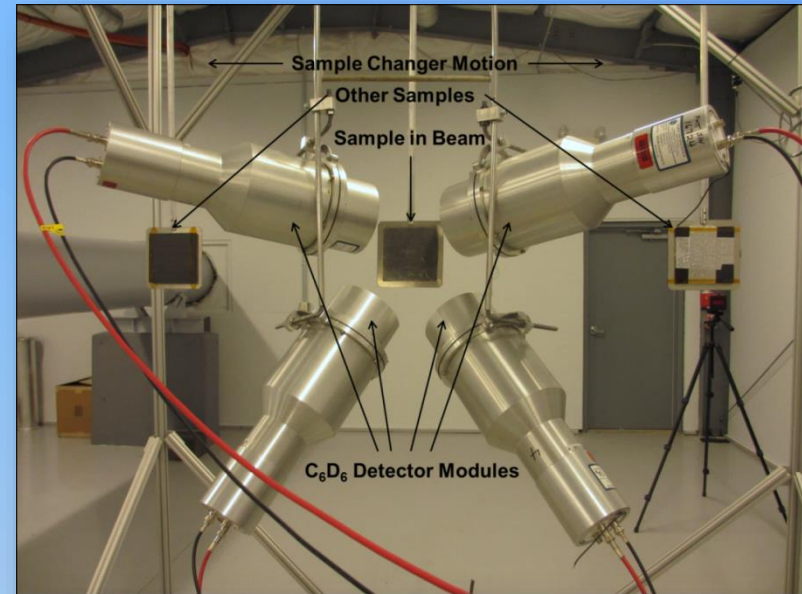


- For measurements of highly scattering resonances in the keV region a different approach is needed
 - Use C_6D_6 detectors
- For keV neutrons better energy resolution is required
 - Translates to longer flightpath



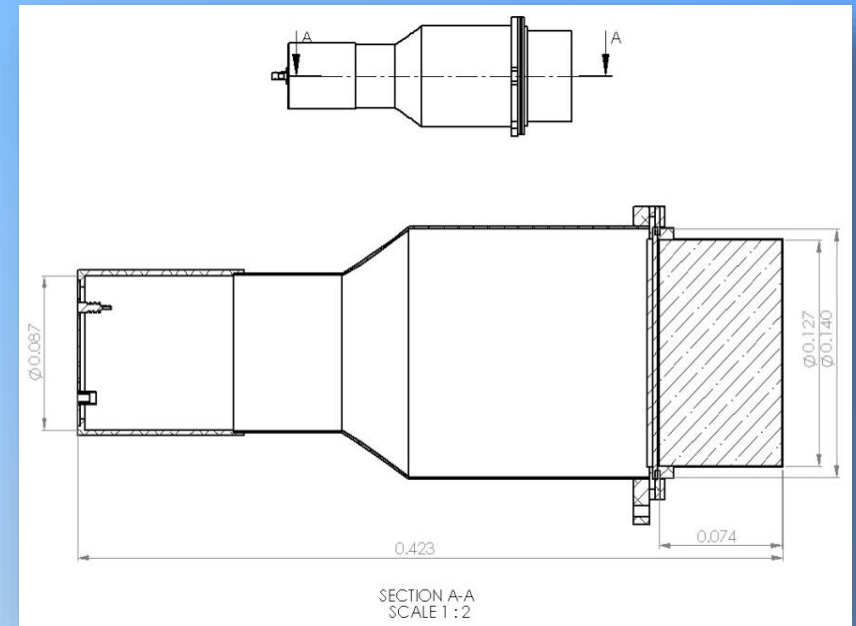
Mid-Energy Capture Detector System Overview

- 4 C_6D_6 detector modules manufactured by Eljen Technology
- **Low mass, low neutron sensitivity design**
- Located at 45m flight path in newly constructed flight station
- Measurements made from 1 eV to 1 MeV



Mid-Energy Capture Detector Design Criteria

- The ideal capture detector meets the following criteria [1,2]:
 1. The efficiency to detect a capture event is independent of the multiplicity and energy distribution of the capture cascade.
 2. The detector is minimally sensitive to the effects of scattered neutrons.
- Additionally, any detection system should have:
 - Good speed and timing resolution
 - Low background
 - High overall detection efficiency

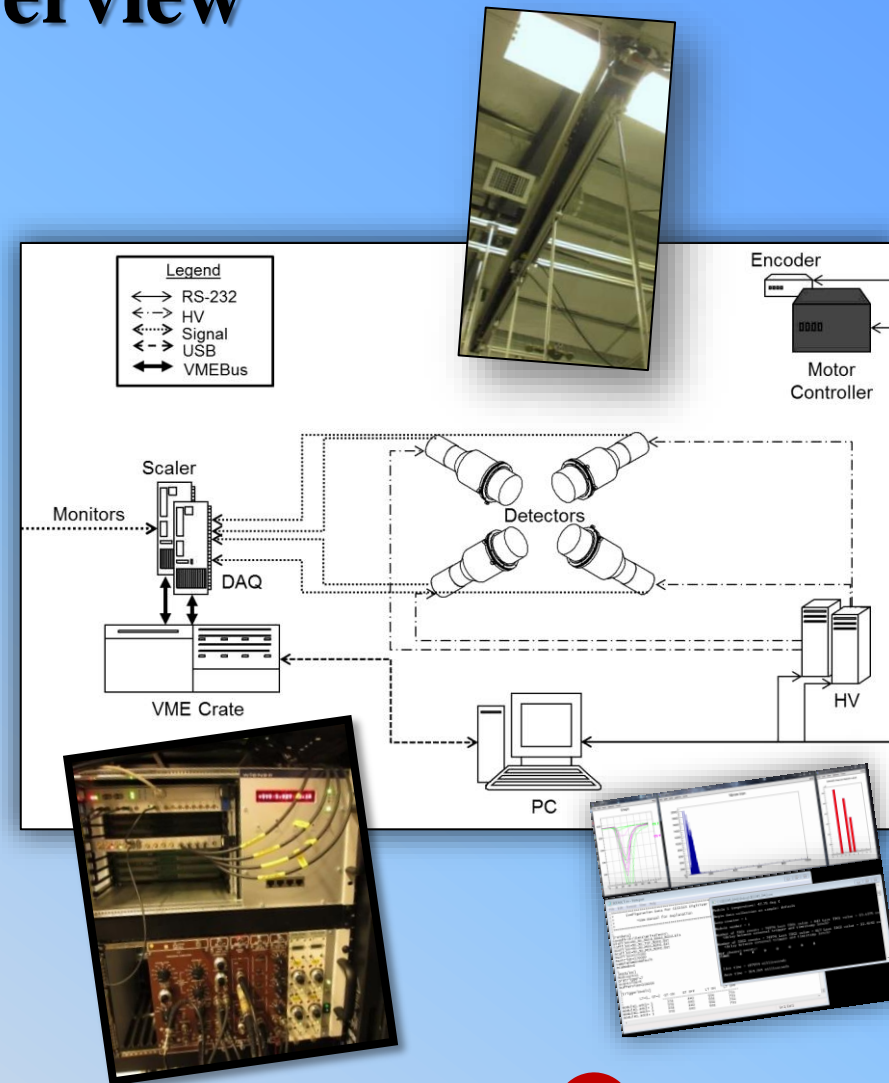


C_6D_6 liquid scintillator

1. A. Borella, G. Aerts, F. Gunsing, M. Moxon, P. Schillebeeckx, and R. Wynants, "The use of C_6D_6 detectors for neutron capture cross-section measurements in the resonance region," Nuclear Instruments and Methods in Physics Research A, vol. 577, pp. 626–640, April 2007.
2. D. Gayther and R. Thom, "Prompt gamma-ray detectors for the measurement of neutron capture cross-sections," in Proceedings Meeting on Fast Neutron Capture, A. N. Laboratory, Ed., April 1982, pp. 205–238.

Mid-Energy Capture Detector System Overview

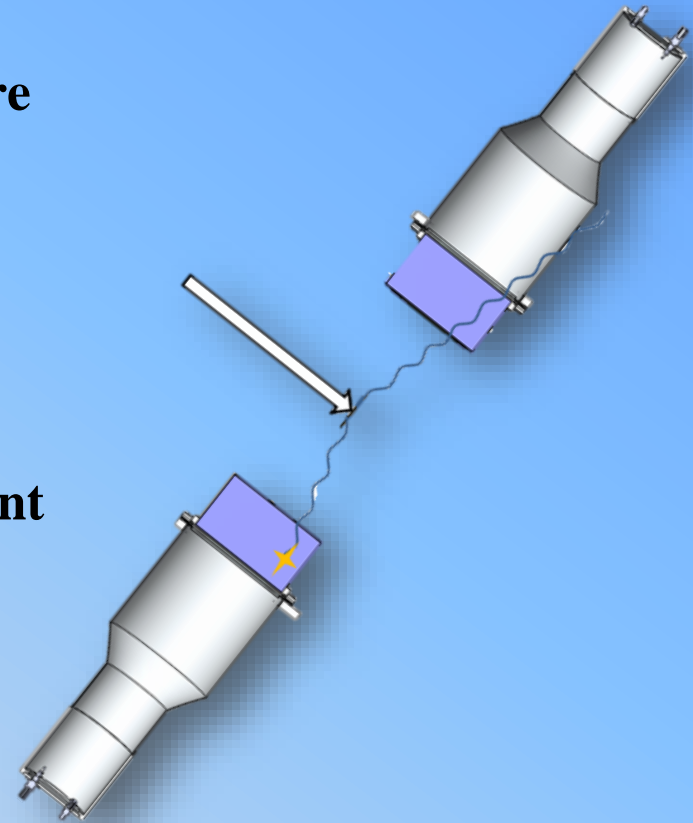
- **Sample Changer**
 - Velmex BiSlide linear translation table w/ stepper motor and magnetic position encoder
- **Data Acquisition**
 - 8-channel SIS3305 digitizer w/ 10-bit, 1.25GHz functionality
- **Beam Flux Monitoring**
 - 8-Channel MDGG-8 Flexible Delay/Gate Generator & Scaler
- **Detector Bias**
 - 2 Dual-channel 3kV NHQ-203M high voltage supplies
- **Software**
 - Custom C/C++ libraries for system control, data acquisition, visualization and data analysis



Mid-Energy Capture Detector Principle of Operation

Uses the “**Total Energy**” detection principle:

1. Detect only a **single photon per capture cascade**
2. Assert that the detection **efficiency is proportional** to the incident photon energy
3. Given 1 and 2, it can be shown that the total **efficiency to detect a capture event is proportional to the total excitation energy** of the compound nucleus, and insensitive to the cascade.



Mid-Energy Capture Detector

“Total Energy” Principle

1. In general, the total detection efficiency for a capture event is given by:

$$\epsilon_c = 1 - \prod_i (1 - \epsilon_{\gamma i})$$

2. For $\epsilon_{\gamma i} \ll 1$:

$$\epsilon_c \approx \sum_i \epsilon_{\gamma i}$$

3. Assert that the efficiency to detect an individual photon be proportional to its energy:

$$\epsilon_{\gamma i} = k E_{\gamma i}$$

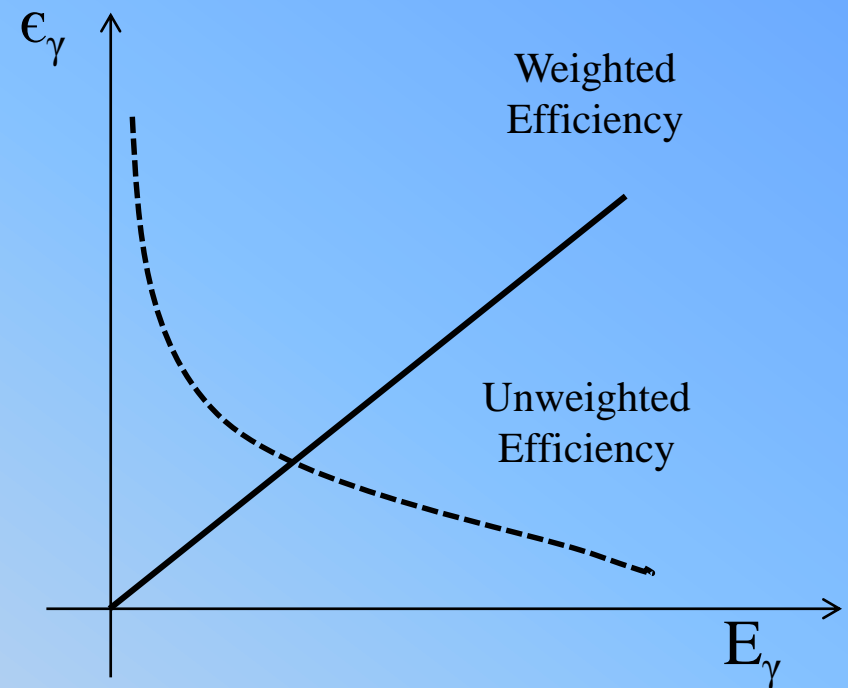
4. Under these assumptions (Eq. 2, 3), the detection efficiency for a cascade is proportional to the *total* excitation energy of the cascade:

$$\epsilon_c \approx k \sum_i E_{\gamma i} \approx k E_x = k(S_n + E_n)$$

ϵ_c	→ Capture Detection Efficiency
$\epsilon_{\gamma, i}$	→ i^{th} Photon Detection Efficiency
$E_{\gamma, i}$	→ i^{th} Photon Energy
E_n	→ Incident Neutron Energy
S_n	→ Neutron Separation Energy
E_x	→ Total Excitation Energy
k	→ Proportionality Constant

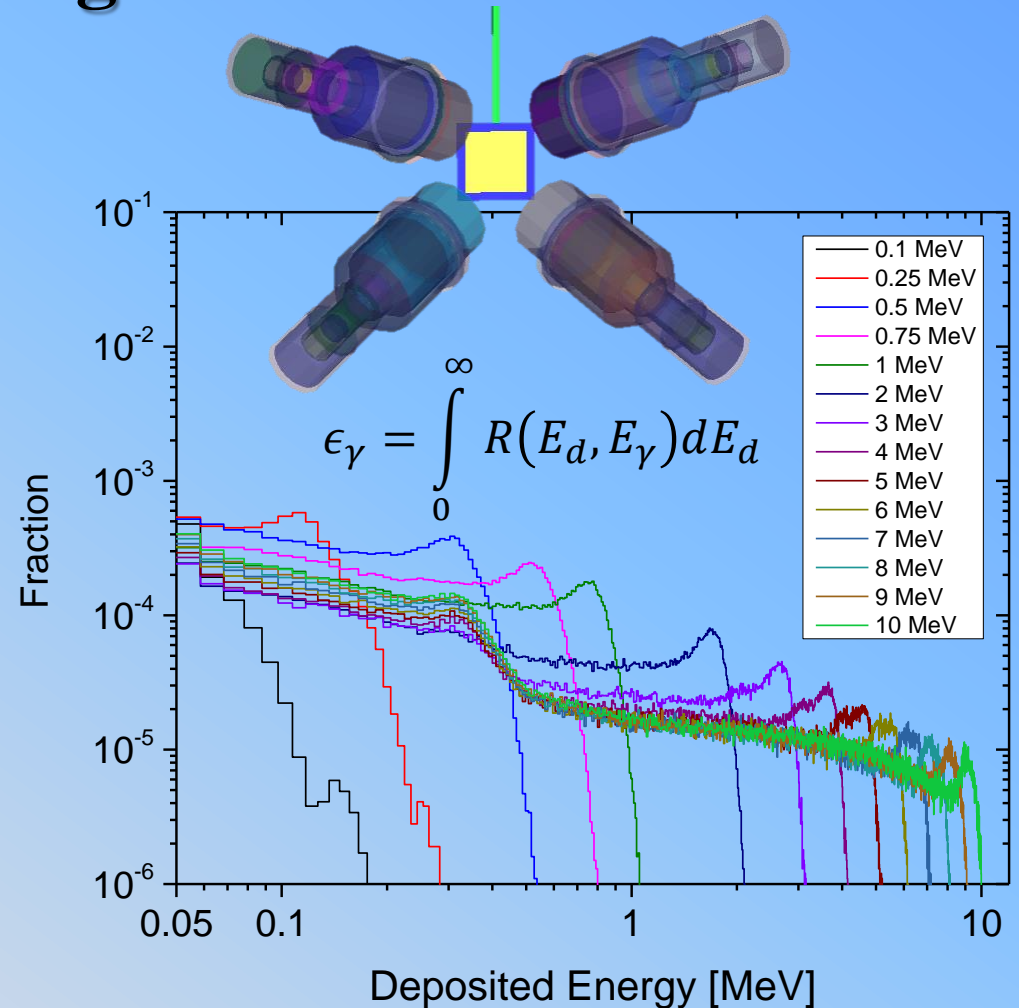
Mid-Energy Capture Detector Need A Weighting Function

- With few exceptions, the efficiency of a detector is not proportional to the incident photon energy.
- A weighting function is applied to the detector response to transform the non-linear efficiency into a linear efficiency
- The weighting function satisfies the proportionality requirement



Mid-Energy Capture Detector Weighting Function

- Weighting functions are sample and source geometry-dependent
- Detector responses from 0.1 to 10 MeV are simulated in MCNP with each sample as a source
- Responses were compared to experimental gamma spectrum of several sources.



Weighting Function I

- For an incident γ -ray with energy E_γ , the probability that it deposits energy E_d is given by the response function:

$$R(E_d, E_\gamma)$$

- Integrating over the response function yields the total detection efficiency for that γ -ray, ϵ_γ :

$$\epsilon_\gamma = \int_0^\infty R(E_d, E_\gamma) dE_d$$

- To satisfy the energy proportionality requirement**, a weighting function $W(E_d)$ is applied to the response function:

$$\epsilon_\gamma = kE_\gamma = \int_0^\infty R(E_d, E_\gamma) W(E_d) dE_d$$

- In terms of the total cascade (m_γ gammas) detection efficiency, this becomes:

$$\epsilon_c \approx k \sum_{i=1}^{m_\gamma} E_{\gamma,i} = \sum_{i=1}^{m_\gamma} \int_0^\infty R(E_d, E_{\gamma,i}) W(E_d) dE_d$$



Obtaining A Weighting Function

$$kE_{\gamma,i} = \int_0^{\infty} R(E_d, E_{\gamma,i})W(E_d)dE_d$$

$$kE_{\gamma,i} = \int_0^{\infty} R(E_d, E_{\gamma,i})(a_iE_d^2 + b_iE_d + c_i)dE_d$$

$$kE_{\gamma,i} = a_i \int_0^{\infty} R(E_d, E_{\gamma,i})E_d^2 dE_d + b_i \int_0^{\infty} R(E_d, E_{\gamma,i})E_d dE_d$$

$$+ c_i \int_0^{\infty} R(E_d, E_{\gamma,i})dE_d$$

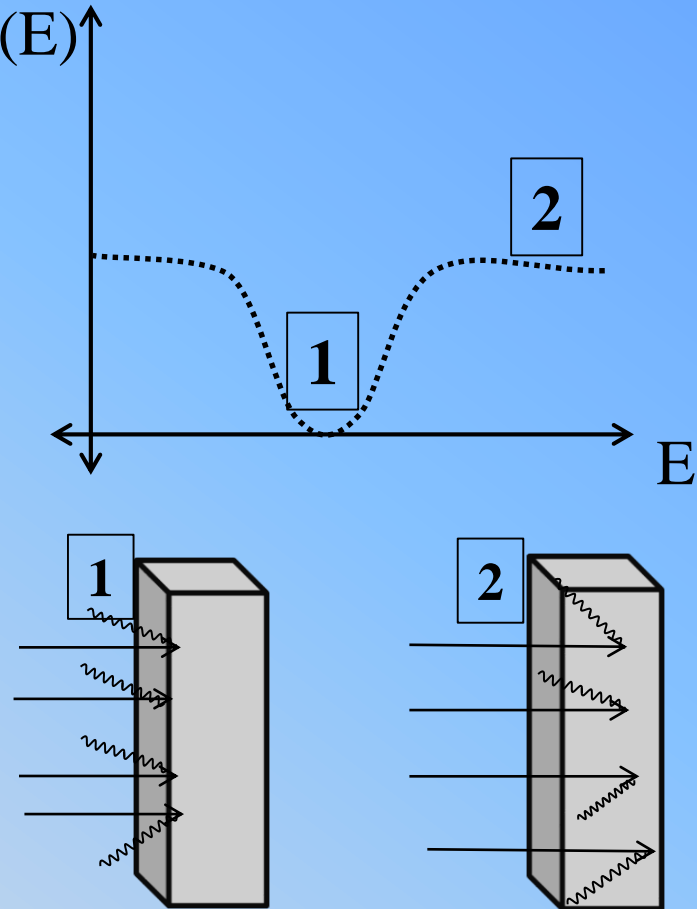
$$\begin{bmatrix} a_1 \int_0^{\infty} R(E_d, E_{\gamma,1})E_d^2 dE_d & b_1 \int_0^{\infty} R(E_d, E_{\gamma,1})E_d dE_d & c_1 \int_0^{\infty} R(E_d, E_{\gamma,1})dE_d \\ \vdots & \vdots & \vdots \\ a_i \int_0^{\infty} R(E_d, E_{\gamma,i})E_d^2 dE_d & b_i \int_0^{\infty} R(E_d, E_{\gamma,i})E_d dE_d & c_i \int_0^{\infty} R(E_d, E_{\gamma,i})dE_d \end{bmatrix} = k \begin{bmatrix} E_{\gamma,1} \\ \vdots \\ E_{\gamma,i} \end{bmatrix}$$

Example: $n = 2$

- Use a polynomial $W(E_d)$
- Use least squares fit to find the polynomial coefficients.
- Use experimental data and MCNP simulations to get the gamma spectrum

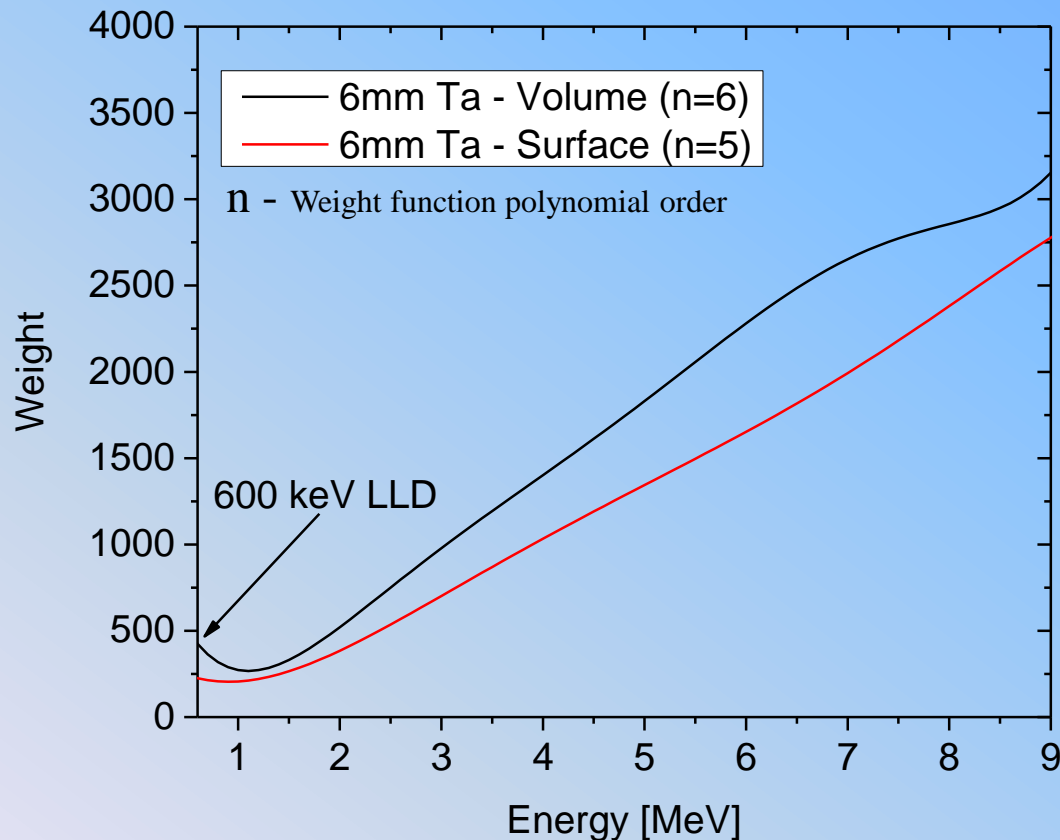
Effect of Sample Thickness on the Weighting Function

- Location of neutron interaction affects the gamma cascade attenuation
- Capture events on the peak of a resonance (where the transmission is low) generate photon cascades near the surface of the sample (1).
- Capture events on the wings of resonances generate photon cascades deeper within the sample (2).
- These differing geometries require a different treatment of the weighting function at different points on the resonance.



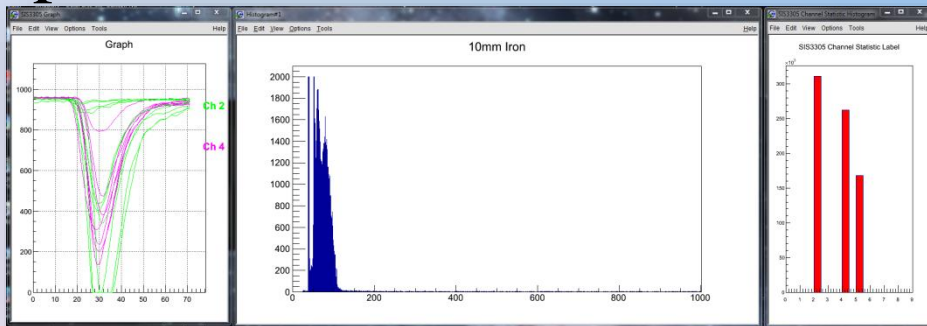
Weighting functions

- Weighting functions for surface capture and volume capture were obtained
 - Surface used for normalization to saturated resonance at 4.2 eV
 - Volume used for weighting the filtered beam data.

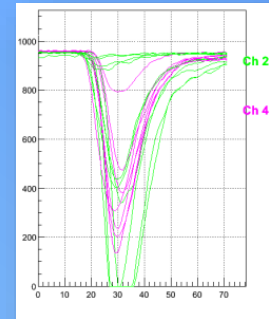


Typical Experiment

- Collect data for a sample of interest
- Collect data with B_4C to obtain the neutron flux shape as a function of time-of-flight.
- Cycle sample and B_4C in and out of the beam every 10 minutes
- Perform online processing to monitor the time-of-flight spectrum



Typical Data Analysis



- For every detected event j in TOF channel i :
 - Obtain the pulse integral $I_{i,j}$
 - Use the energy calibration to obtain $E_{i,j}$
 - Sum all weighted events for the sample C^s , its background C^{sB} , the flux C^ϕ , and its background $C^{\phi B}$:

$$C_i^x = \sum_j^{n \text{ events}} W(E_{i,j}) \quad \text{non weighted case: } C_i^x = \sum_j^{n \text{ events}} 1$$

- Calculate the capture Yield:

$$Y_i^s = \frac{C_i^s - C_i^{sB} \frac{m^s}{m^{sB}}}{C_i^\phi \frac{m^s}{m^\phi} - C_i^{\phi B} \frac{m^s}{m^{\phi B}}} n \quad \text{Where } m^x \text{ are the beam monitor counts}$$

- Normalize the yield (find n)
 - To a known black resonance, or to a transmission measurement.

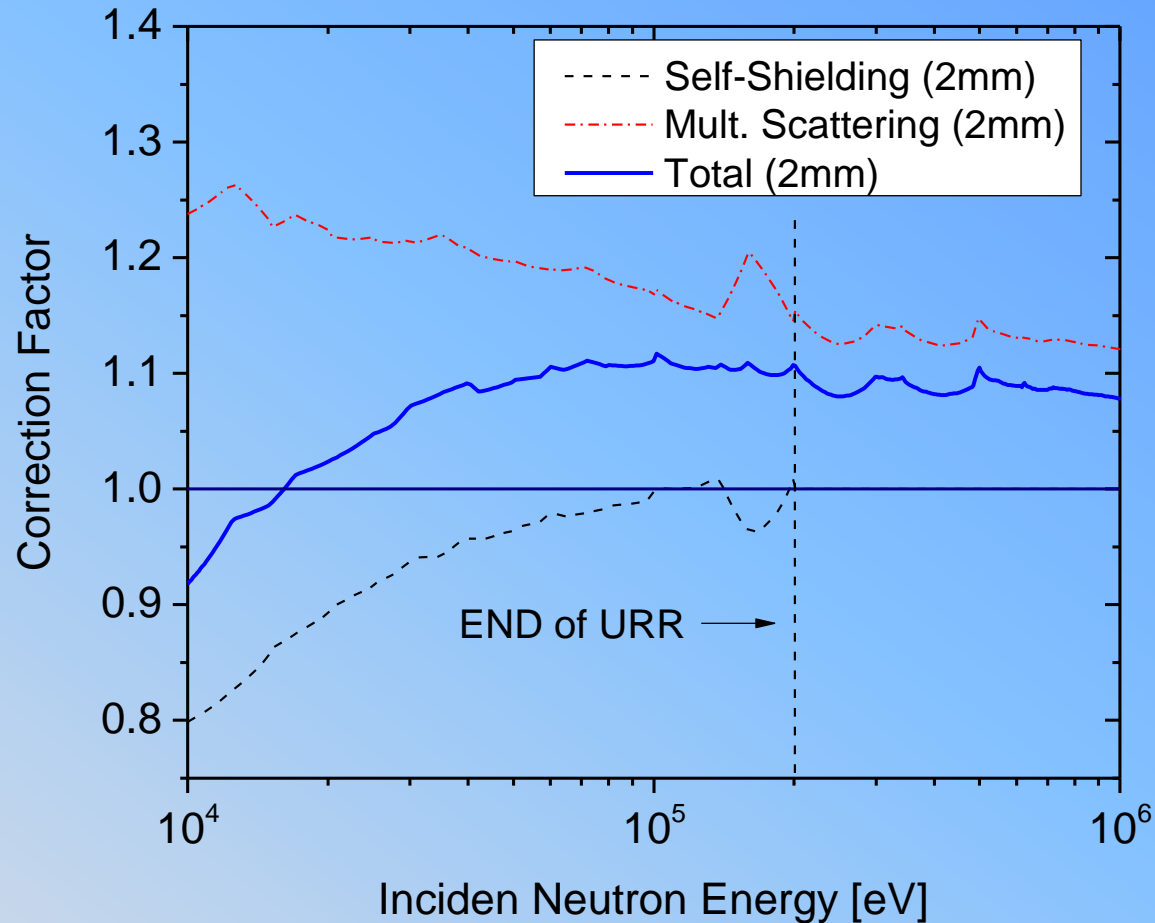
Corrections to the URR Measured Capture Yield

- In the URR corrections for two effects are needed:
 - Multiple scattering (results in observed higher yield)
 - Self shielding (results in observed lower yield)

- The experimental yield is corrected to obtain the cross section.

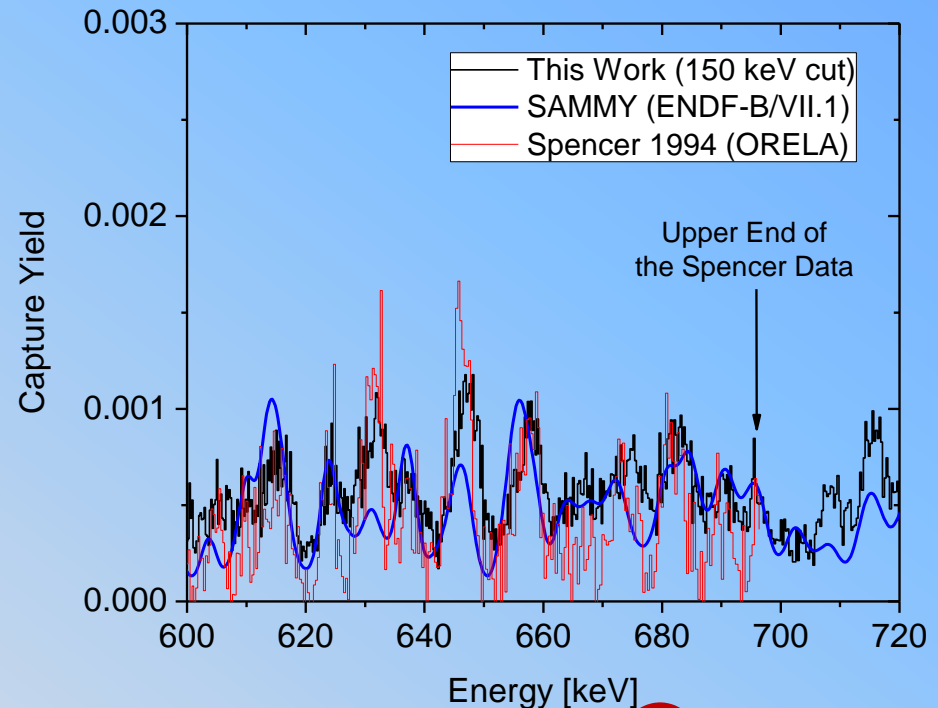
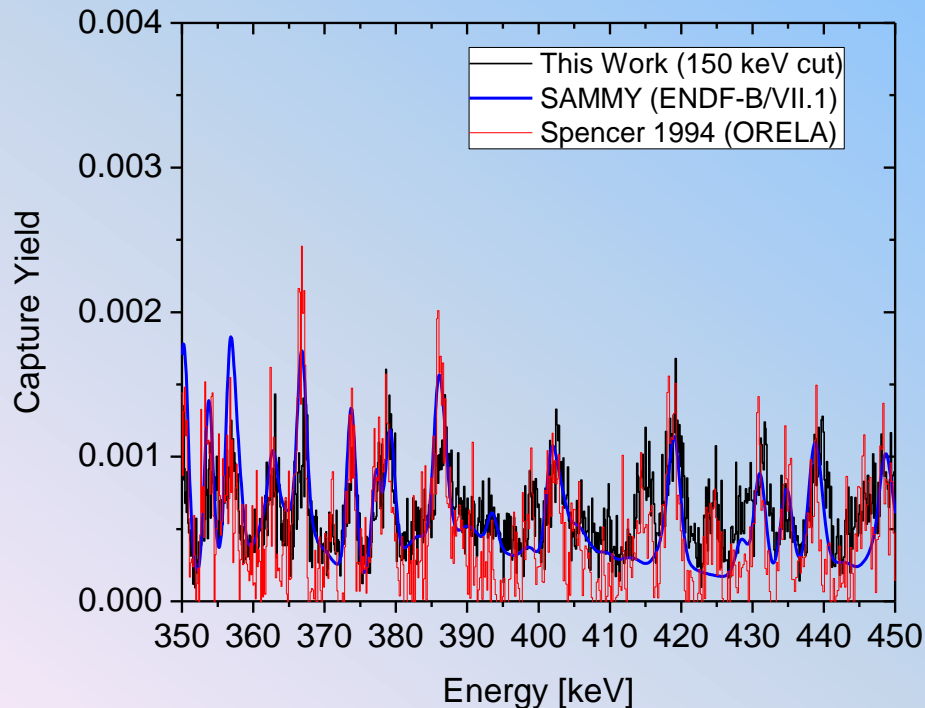
$$\sigma_{\gamma} = \frac{Y_{exp}}{N \cdot C} n$$

- Where N is the number density, C the correction factor and n normalization
- The correction works better for thin samples that minimize the self-shielding and multiple scattering



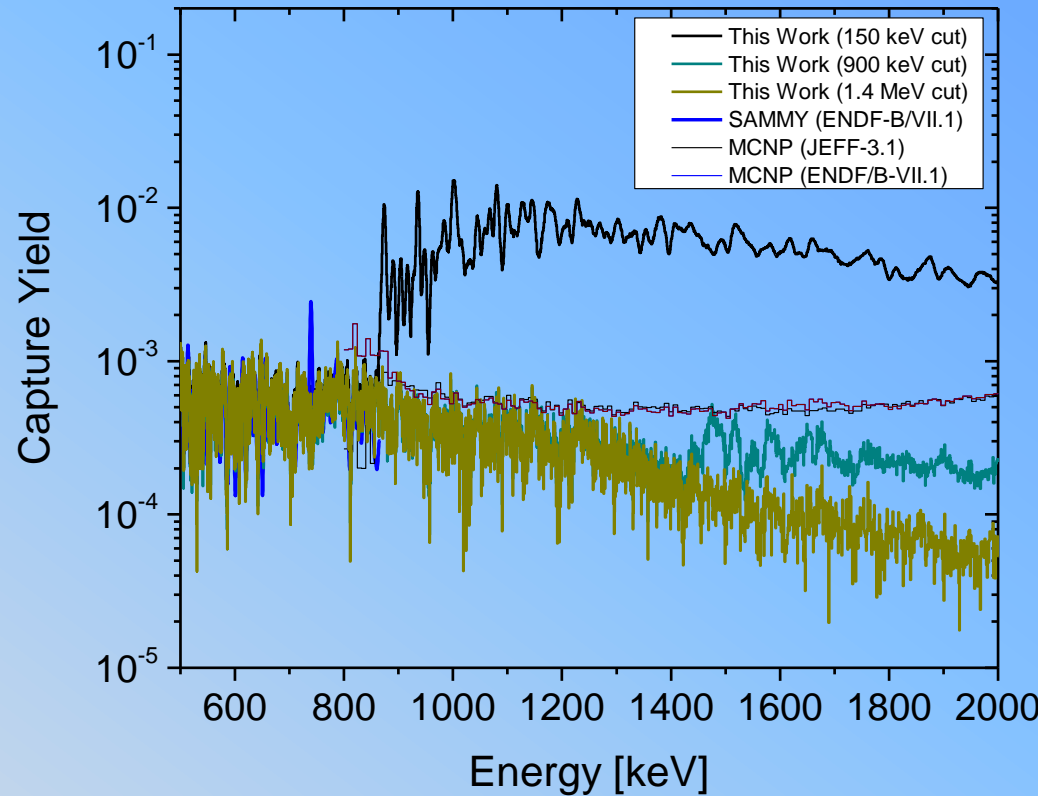
Fe Capture

- Iron was used as a test to compare with evaluations and other measurements
 - The RPI data (45m flight path) has good energy resolution compared to the Spencer ORELA data (40m flight path)
 - The RPI data provide information above 700 keV



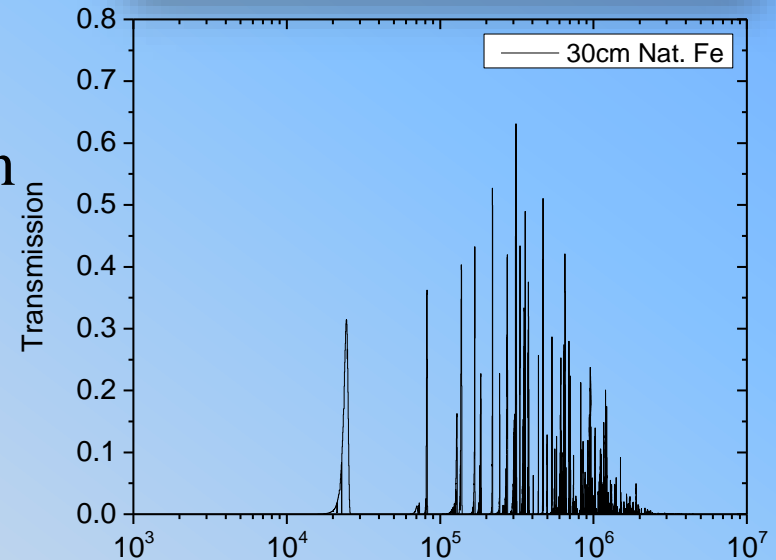
Mid-Energy Capture Detector Experimental Results-^{nat}Fe

- New capture data obtained above 847 keV and 1409 keV inelastic states in ⁵⁶Fe and ⁵⁴Fe
- Capture signal separated from inelastic scattering signal by post-processing digitized waveforms with different energy deposition cutoffs



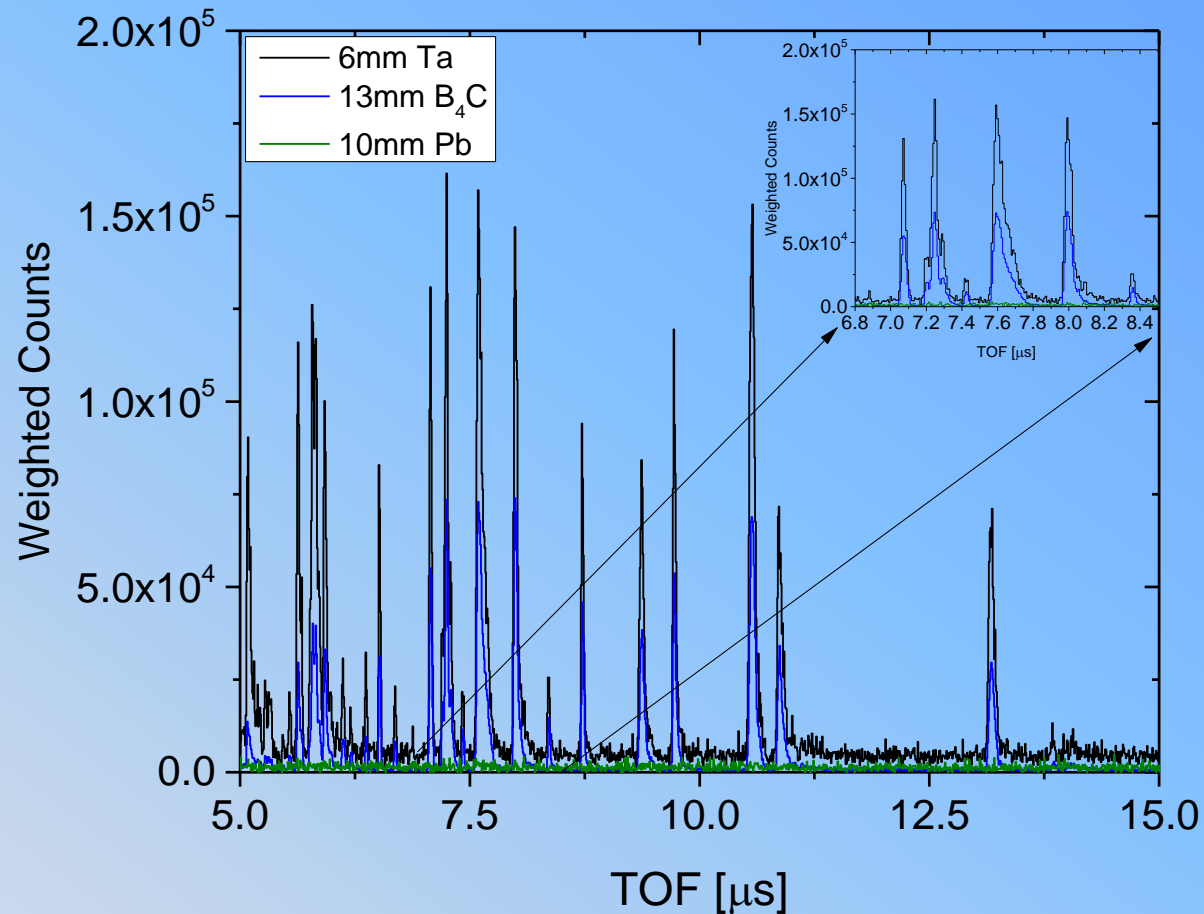
New Method – Fe Filtered Beam Capture Results for ^{181}Ta

- Measurements performed on ^{181}Ta using Fe-filtered beam technique
- 30cm thick Fe filter removes all beam-related gamma and neutron background
- Provides a quasi-monoenergetic neutron source corresponding to deep minima in the Fe cross section



Mid-Energy Capture Detector Experimental Results-¹⁸¹Ta

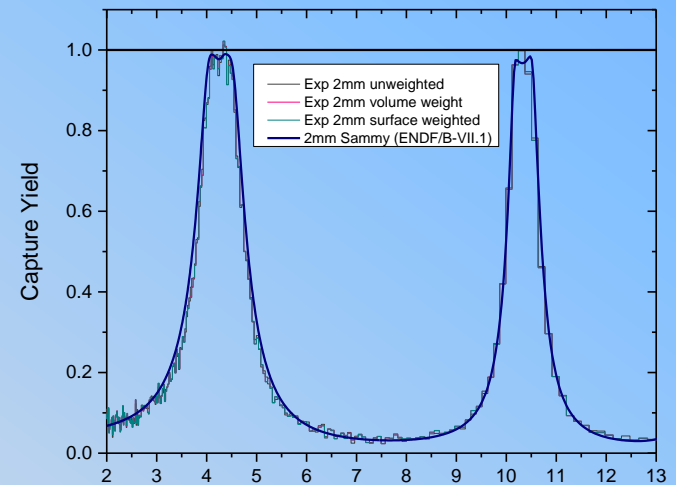
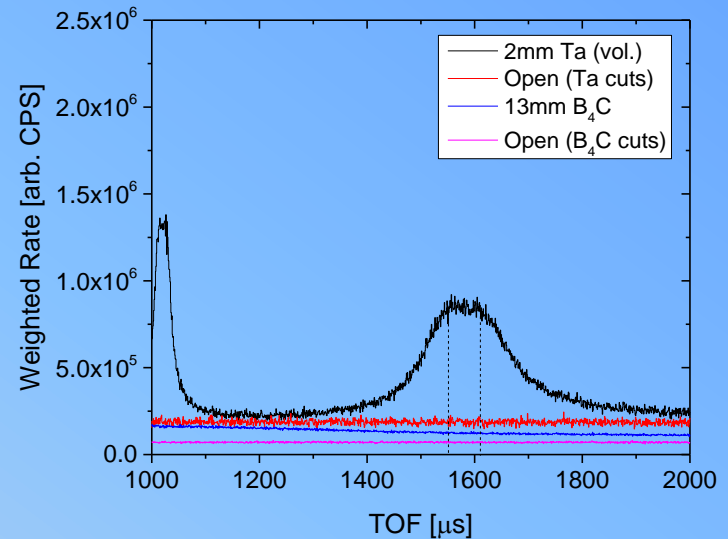
- Count rates for Ta and B₄C samples were summed under each filter transmission peak.
- Pb scattering sample used to confirm negligible neutron background



Mid-Energy Capture Detector

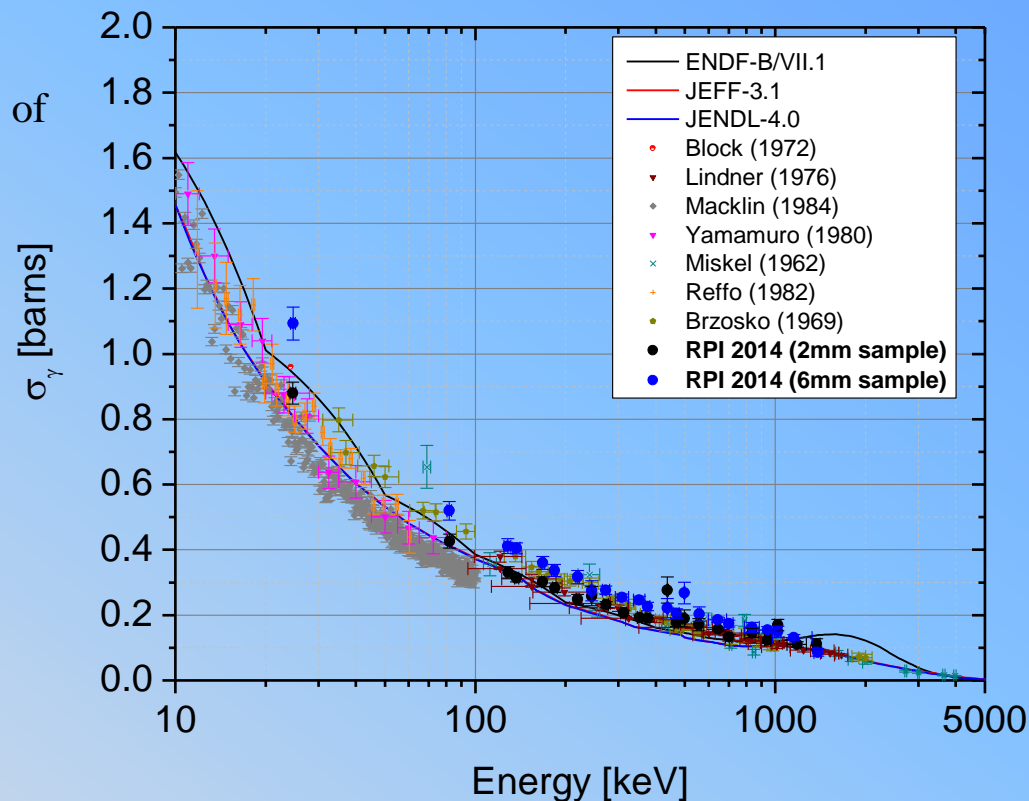
Experimental Results- ^{181}Ta Normalization

- Unfiltered run performed to determine normalization factor from 4.2 eV saturated resonance
- Normalization factor determined from the ratio of B_4C to Ta counts at the location of the saturated resonance ($Y_\gamma \approx 1$)
- A refinement of the normalization is based on a SAMMY calculations



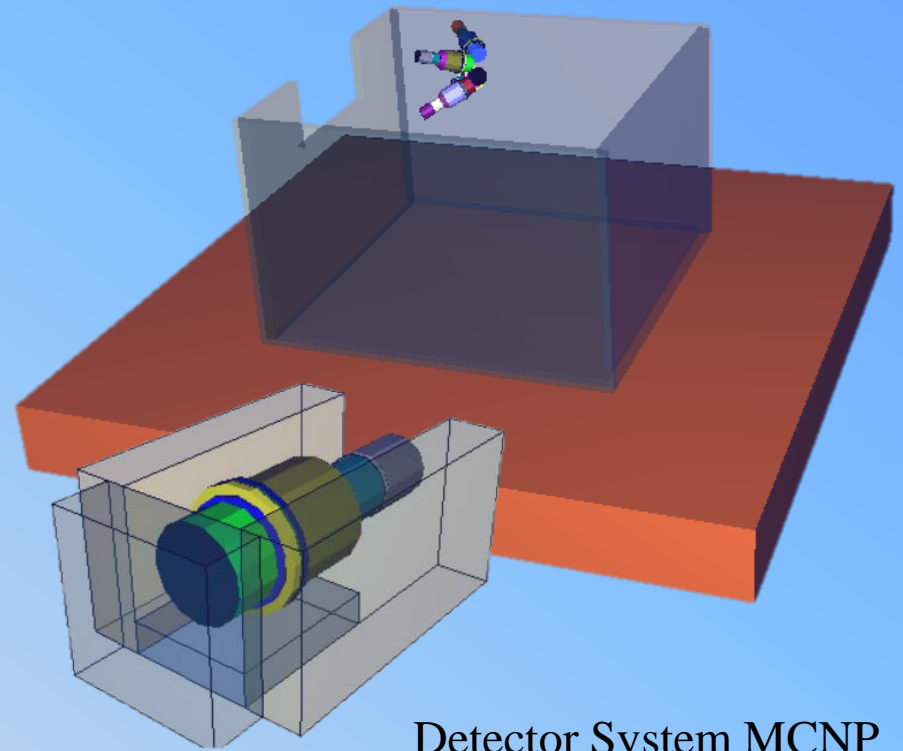
Experimental Fe Filtered Beam Results: ^{181}Ta

- As expected thick sample=problems
 - Self shielding correction is high
 - Multiple scattering correction is high
 - Need to work on better understanding of the weighting function and its validity
- Thin sample support the JEFF-3.1/3.2 evaluation
- Possible contamination from inelastic scattering apparent in ENDF/B-VII.1

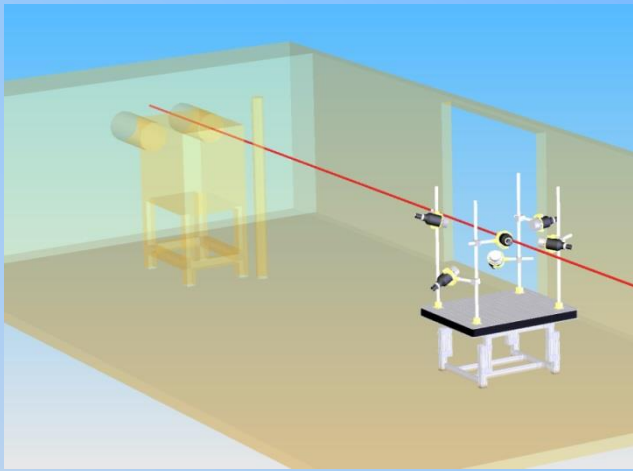


Mid-Energy Capture Detector Future Work

- Complete development of the data analysis methods
- Complete analysis and publication of Fe and Ta work
- Explore and implement options for reducing ambient background
- Improve the mechanical stability of the detector array



Detector System MCNP
Shielding Geometries

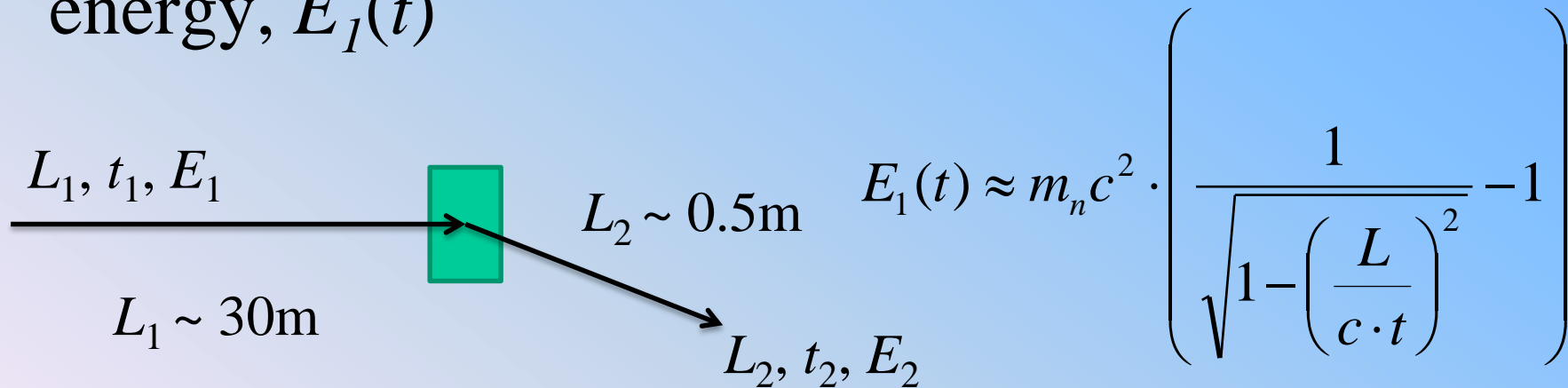


Neutron Scattering From ^{nat}Fe



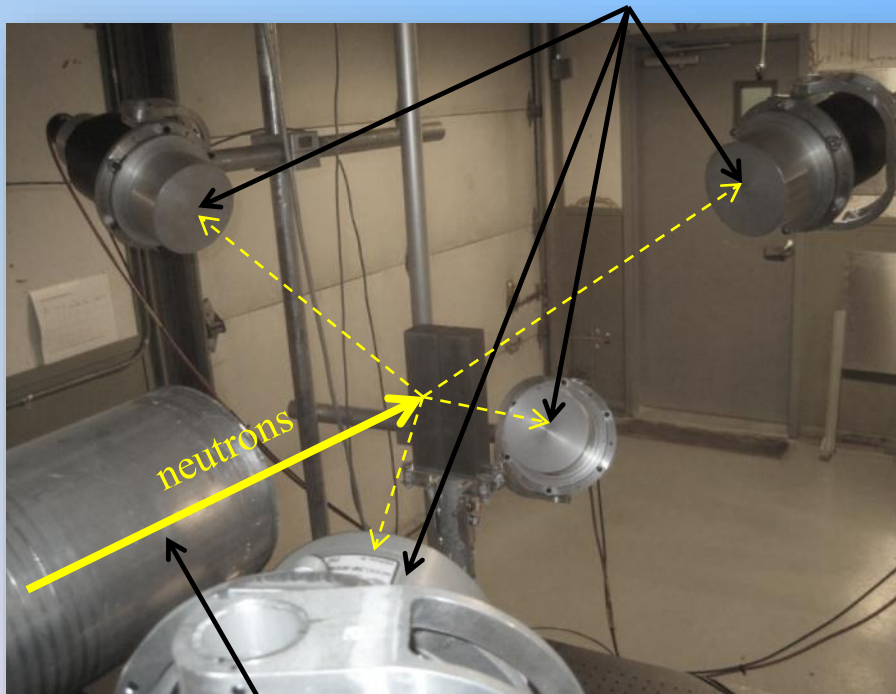
TOF Scattering Measurement

- Measure TOF: $t = t_1 + t_2$; where $t_1 \gg t_2$
- All scattering events: $E_2 < E_1$
- For elastic scattering with $A \gg 1$: $E_1 \sim E_2$
- Assuming $L = L_1 + L_2$ than total TOF, t , can be used to calculate the incident neutron energy, $E_1(t)$



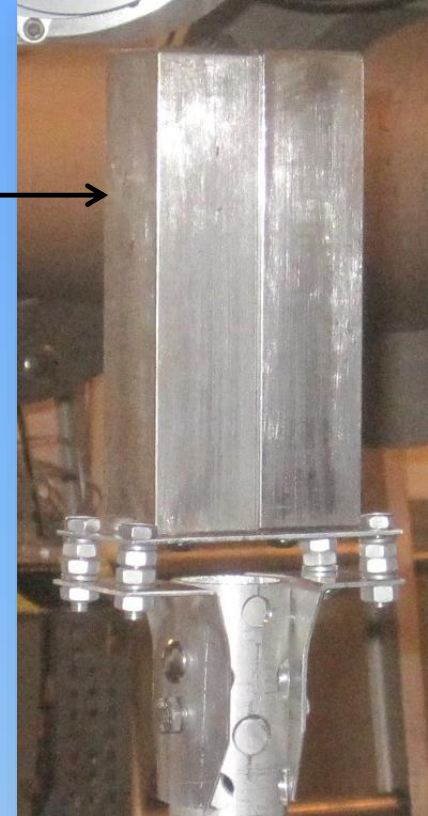
Fe Scattering Measurement - Setup

EJ-301 Liquid Scintillator Neutron Detectors



Evacuated Flight Tube

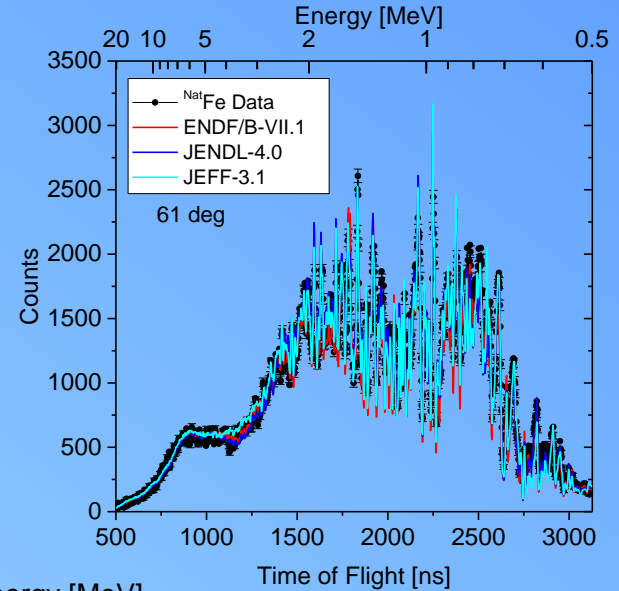
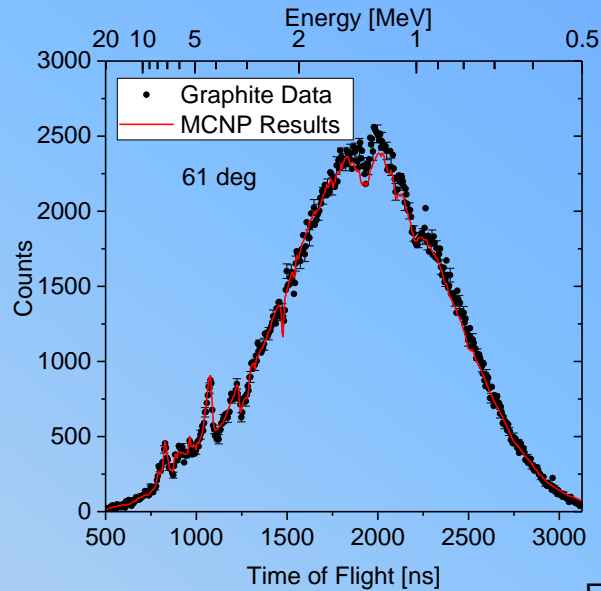
- Fe Sample
- Dimensions 77.0 x 152.6 x 32.2 mm



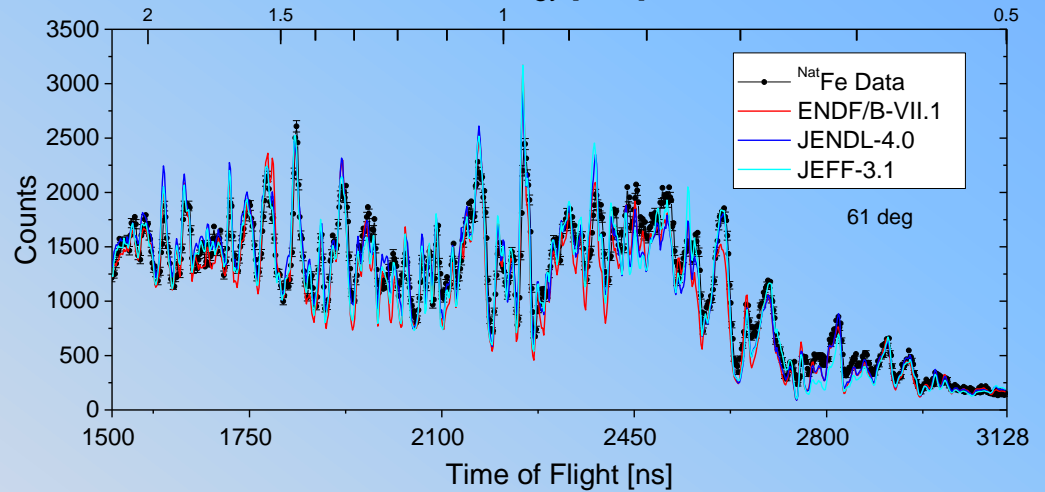
The neutron beam size is smaller than the sample.

^{nat}Fe Scattering - 61°

Reference	FOM
Graphite	1.20



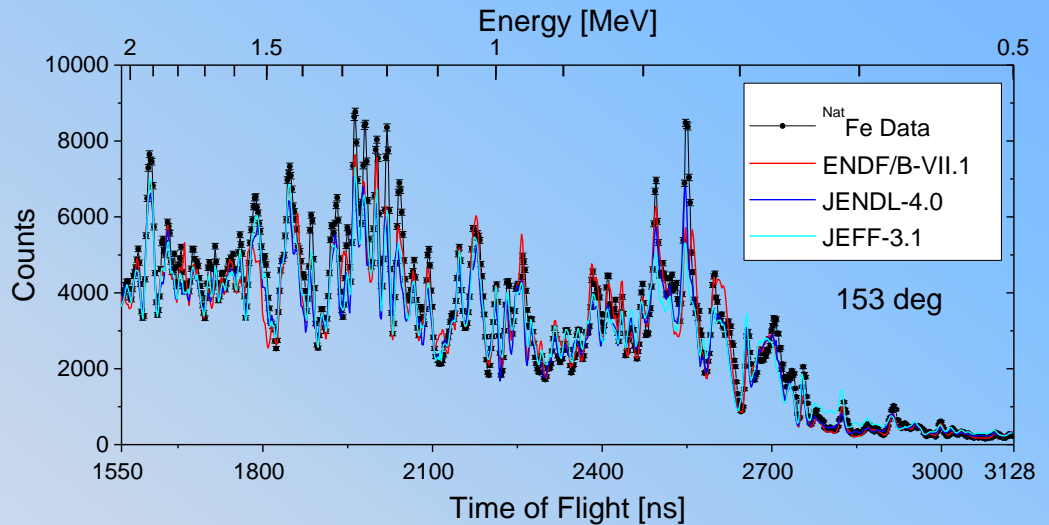
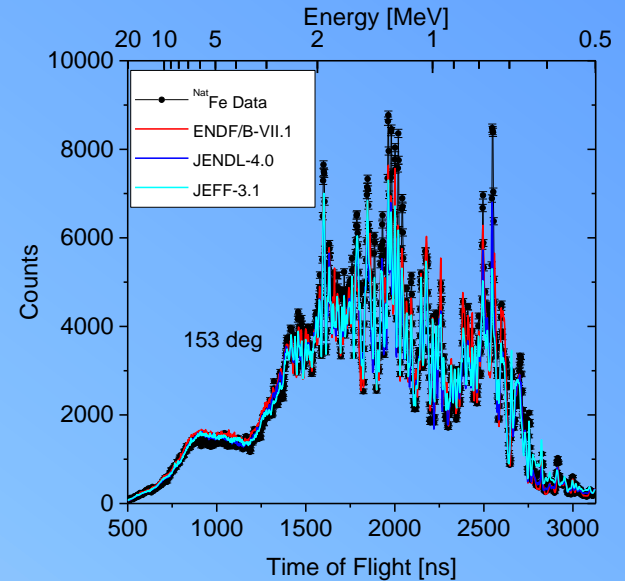
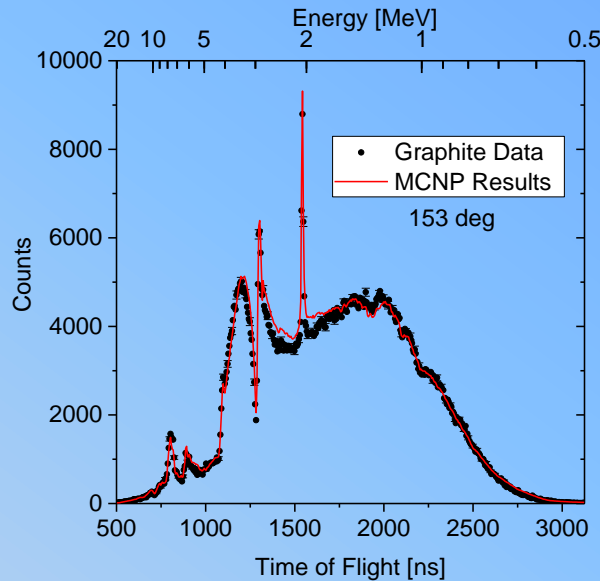
Library	FOM
ENDF/B-VII.0	13.67
JEFF-3.1	13.45
JENDL-4.0	10.97



^{nat}Fe Scattering - 153°

Reference	FOM
Graphite	1.94

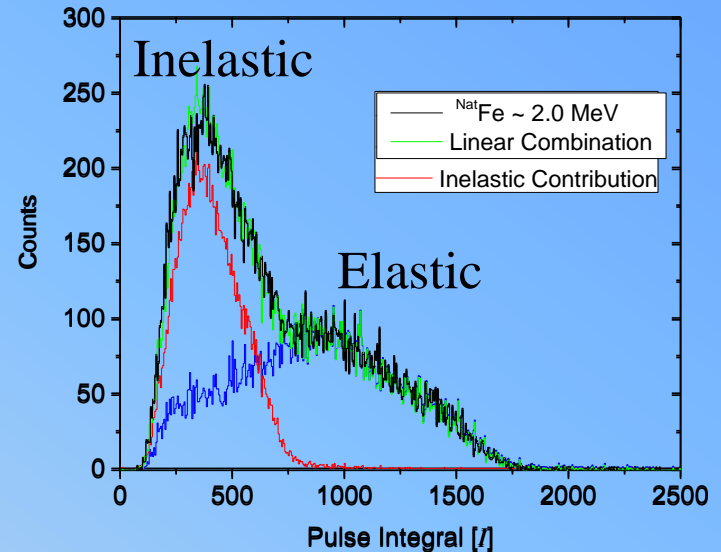
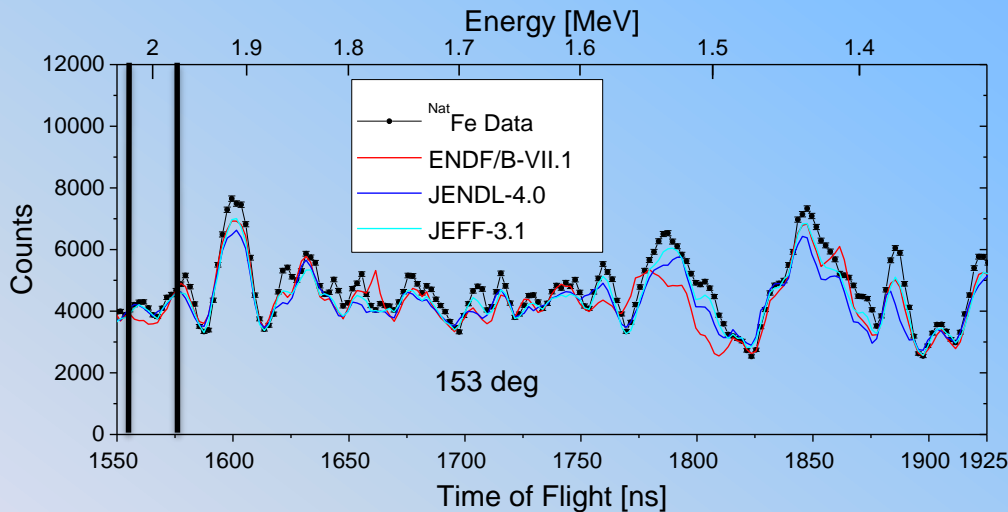
Library	FOM
ENDF/B-VII.0	14.42
JEFF-3.1	20.31
JENDL-4.0	14.68



Observations for ^{Nat}Fe

- The JENDL-4.0 evaluation had best overall agreement with experimental data from 0.5 to 20 MeV with all angles.
- Experimental data can be analyzed further to provide:
 - Inelastic to Elastic Scattering Ratios
 - Elastic (only) Scattering Contribution

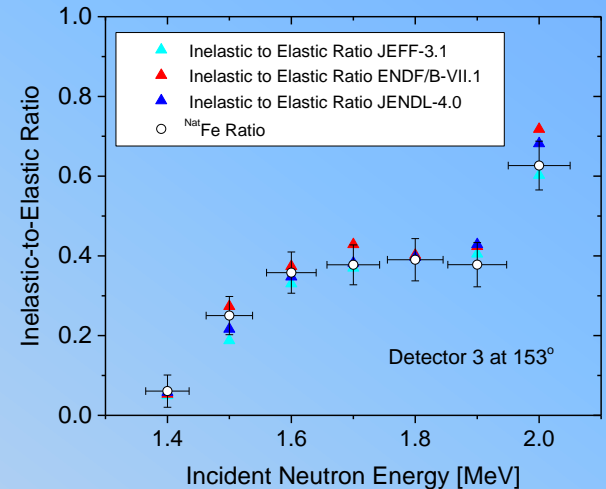
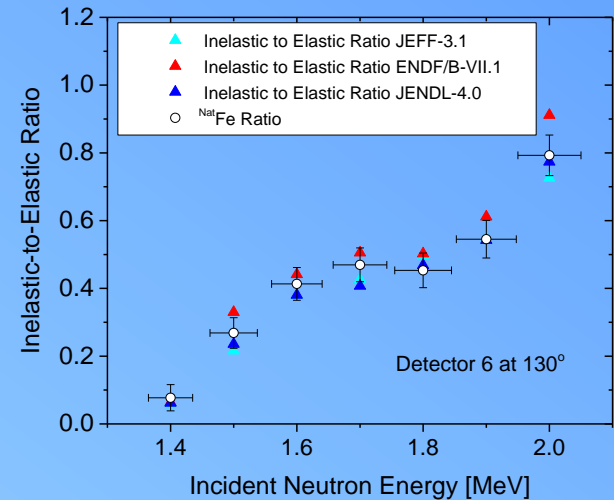
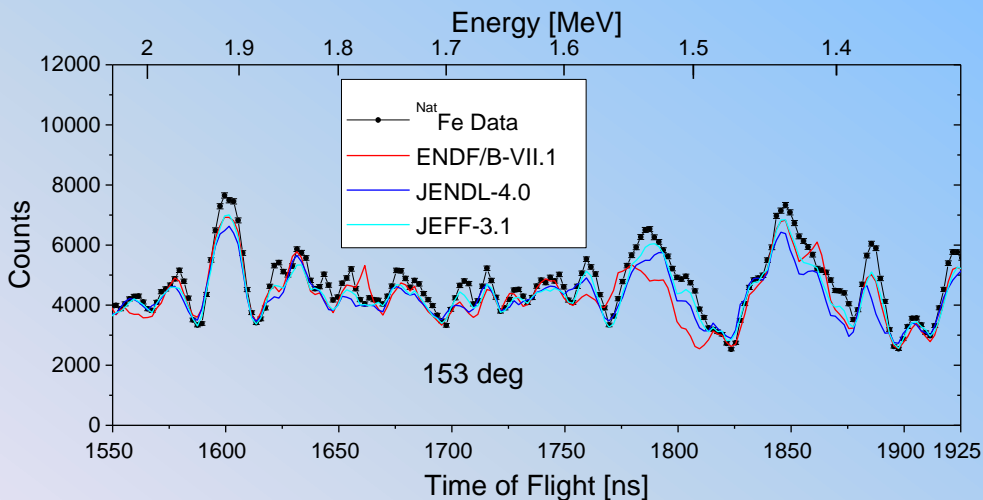
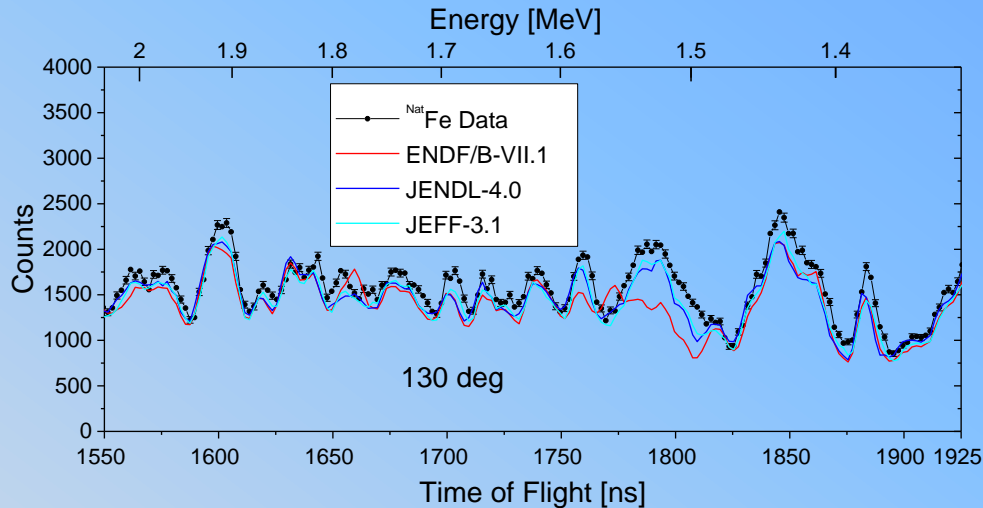
Inelastic to Elastic Ratio ^{Nat}Fe



- Select an energy region (shown between the two black vertical)
- Fit in-beam response functions, $f_{el}(I)$ and $f_{inl}(I)$, to known levels

$$\text{Response}(I) = A \cdot f_{el}(I) + (1 - A) \cdot f_{inl}(I) \quad \text{Ratio} = \frac{(1 - A)}{A} \quad A - \text{Fitted elastic fraction}$$

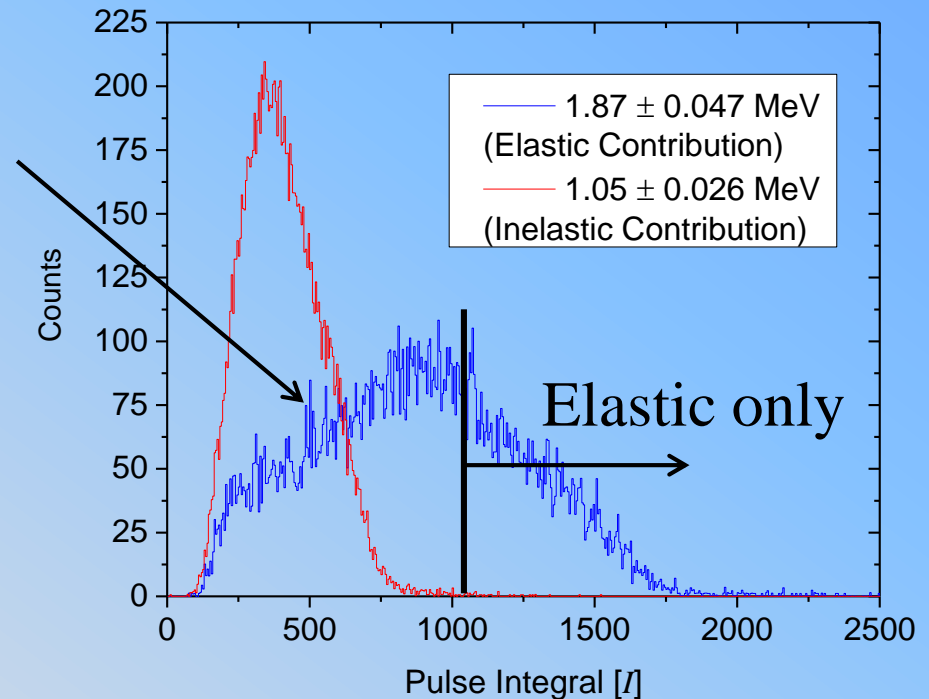
Inelastic to Elastic Ratio



- Multiple scattering effects included in MCNP simulations
- Statistical and systematic uncertainties included in analysis

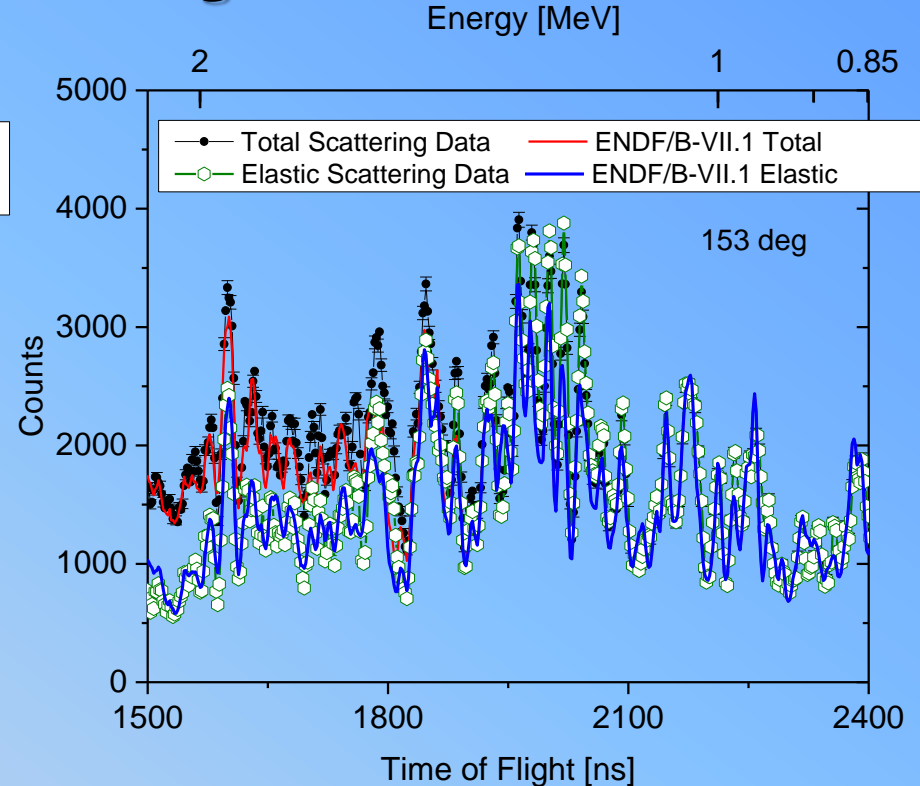
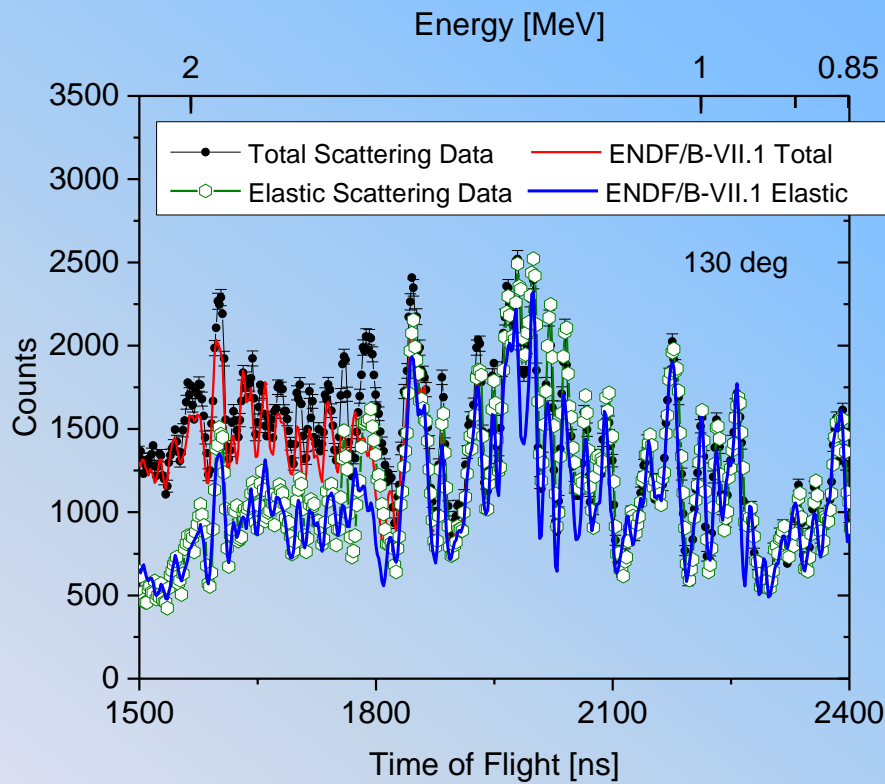
Elastic Scattering Contribution

- Isolate only the elastic scattering:
 - Cut pulses with integral less than the discrimination.
 - Correct for the elastic shape that was discriminated.
- The contribution of elastic scattering below the discriminator leave can be corrected for.
- Use the know pulse height shape.



Comparing Experiments and Simulation

Elastic scattering



- Experimental elastic scattering was inferred from 0.5 to 2.0 MeV
 - The experimental data is reasonably represented by a simulation with ENDF/B-VII.1
- Collaborating with ORNL to improve new ^{56}Fe evaluation

LINAC 2020 Refurbishment and Upgrade Plan

- SLAC team delivered:
 - Design concept for the layout of the accelerator.
 - Initial modulators design parameters
- An order for 5 Thales klystrons was sent to the vendor.
- Planned for FY16
 - Modulators order
 - Accelerator sections design.



Past Year Accomplishments

- Developed a new capability to measure capture cross sections in the mid energy (keV) range
 - Performed a capture measurement for Ta and Fe samples.
 - Developed methods to generate weighting function and multiple scattering corrections in the URR.
 - Developed a new method for filtered beam capture cross section measurements in the URR
- Fast neutron scattering measurements
 - Completed analysis of fast neutron scattering from Iron
 - Obtained ratio of inelastic to elastic cross section for the first excited state.
 - Generated elastic scattering only data.
 - Delivered data to ORNL for inclusion in extension of RRR above 847 keV.
- LINAC 2020 refurbishment and upgrade plan in progress
 - Order for Klystrons was placed with Thales.
 - Developing the specifications for the replacement modulators

